ACCEPTED VERSION

http://hdl.handle.net/2440/74065

Triazolium containing MOFs: Control of Catenation in 2-D Copper(II) Paddlewheel Structures

Alexandre M. Burgun,[A] Christian J. Doonan,[A] and Christopher J. Sumby[A,B]

[A] School of Chemistry and Physics, University of Adelaide, Adelaide, SA 5005, Australia.

[B] Corresponding author. Email: christopher.sumby@adelaide.edu.au

Abstract

One approach to exploit MOFs as heterogeneous catalyst platforms requires the development of materials containing groups that can be utilised to anchor a catalytic moiety into the links within the structure. Here we report the synthesis of the first integrated triazolium-containing MOF linker and the first MOFs containing linkers of this type. 1,4-Bis(4-benzoic acid)-1-methyl-1H-1,2,3-triazolium chloride, H$_2$**L1**^{Me}, was synthesised in three steps by a 'Click' reaction of methyl 4-ethynylbenzoate with methyl 4-azidobenzoate, methylation using methyl triflate, followed by ester hydrolysis in overall 74% yield. The equivalent neutral triazole precursor, 1,4-bis(4-benzoic acid)-1H-1,2,3-triazole hydrochloride, H$_2$**L1**(HCl), was also prepared and a comparison of the chemistry with Zn(NO$_3$)$_2 \cdot$6H$_2$O and Cu(NO$_3$)$_2 \cdot$3H$_2$O is presented. [Zn(**L1**)$_2$(H$_2$O)$_2$] is a 2-D MOF with infinite chains of zinc carboxylates bridged by **L1**, while an equivalent structure is not observed for **L1**^{Me}. In turn, two catenation isomers of [Cu$_2$(DMF)$_2$(**L1**^{Me})$_2$](NO$_3$)$_2$ were isolated from a single reaction of **L1**^{Me} and Cu(NO$_3$)$_2 \cdot$3H$_2$O. The α-form, a close-packed 3-fold interpenetrated structure, was obtained from reactions undertaken in the presence of nitric acid or at lower temperatures, while undertaking the reaction at higher temperatures leads to a predominance of the 2-fold interpenetrated and potentially porous β-form of the structure. The work presented provides further support for the use of reaction conditions to control interpenetration and additional evidence that charge on structurally similar ligands can drastically alter the types of structures that are accessible due to the requirements for charge balance in the final product.

Introduction

Metal-organic frameworks (MOFs) or porous coordination polymers (PCPs) are porous extended networks that can be synthesised from a systematic combination of organic links and metals or metal oxide clusters.[1] By judicious choice of both precursor metal salt and organic ligand, materials with varying topologies; pore sizes, shapes and chemistry; and properties can be synthesised.[2] Due to the exquisite control that can be imparted during synthesis, their large pore volumes and stable structures, MOFs have been identified as materials with great potential for size-selective heterogeneous catalysis.[3] By virtue of these rational design principles the desirable properties of homogeneous catalysts can be transferred to a heterogeneous MOF platform. One approach to exploit MOFs as heterogeneous catalysts is to construct the organic backbone of the material from links capable of anchoring a known homogeneous catalyst. However, such an approach requires a number of challenges to be overcome. Firstly, MOFs with pores sufficiently large enough to concurrently allow anchoring of the catalyst, diffusion of chemical reactants through the pore structure, and to facilitate a catalytic transition state are required. Secondly, reliable methods for anchoring catalytic moieties to the framework need to be established that do not result in unwanted side reactions during MOF synthesis or hinder the formation of the desired network topology. This second challenge is the focus of this contribution.

A number of examples of MOFs containing non-structural functional groups have been reported. These include the inclusion of 2,2'-bipyridine and pyridyl imine motifs,[4] cyclometallating moieties,[5] phosphines,[6] and other coordinating sites,[7] such as diols.[8] In a number of cases, these require judicious choice of the structural metal,[4a] post synthetic modification,[4b] or protecting groups,[8e] to prevent the secondary functional groups from being used to form a non-desired framework. Azoliums, precursors to N-heterocyclic carbenes, have also been investigated with a view to generating catalytically competent MOFs.[9, 10, 11]

Recent examples of azolium containing ligands have all been based on an imidazolium[9, 10] or a benzimidazolium[11] precursor to the N-heterocyclic carbene. The imidazolium containing ligands for MOF synthesis have come in two forms; the first where the azolium is integrated into the backbone of the ligand,[9] and the second, where the azolium moiety is incorporated pendant to the link.[10] Examples of the latter class were recently reported by Hupp and Scheidt[10] involving 4,4'-biphenyldicarboxylates appended with one or two azolium groups in the 2 and 2' positions of the biphenyl (**1a** and **1b**, respectively). These provided for the synthesis of IRMOF-9 and IRMOF-10 analogues with $Zn(NO_3)_2 \cdot 6H_2O$ depending on whether the ligand contained two or one azolium groups respectively.[10] The first reports of an imidazolium containing linker concerned the use of a flexible ligand, N,N'-diacetic acid imidazolium chloride (**2**).[9a-c] We,[9d] Chun *et al.*,[9e, 9f] and Hupp[9g] have also reported frameworks based on more rigid linkers where an imidazolium is part of the link (**3** – **6**), which confers an unusual zeolite-like geometry on the link component in these structures. Finally, Yaghi[11] reported a system partway between these extremes by using a benzimidazolium core to generate a linear dicarboxylate (**7**) whereby the azolium was integrated into the link backbone of a cubic MOF. More recently a linker with two azolium groups in the backbone (**8**) was used to synthesis a 2-D MOF network consisting of 80-membered macrocycle rings of **8** bridging copper paddle-wheel subunits.[9h]
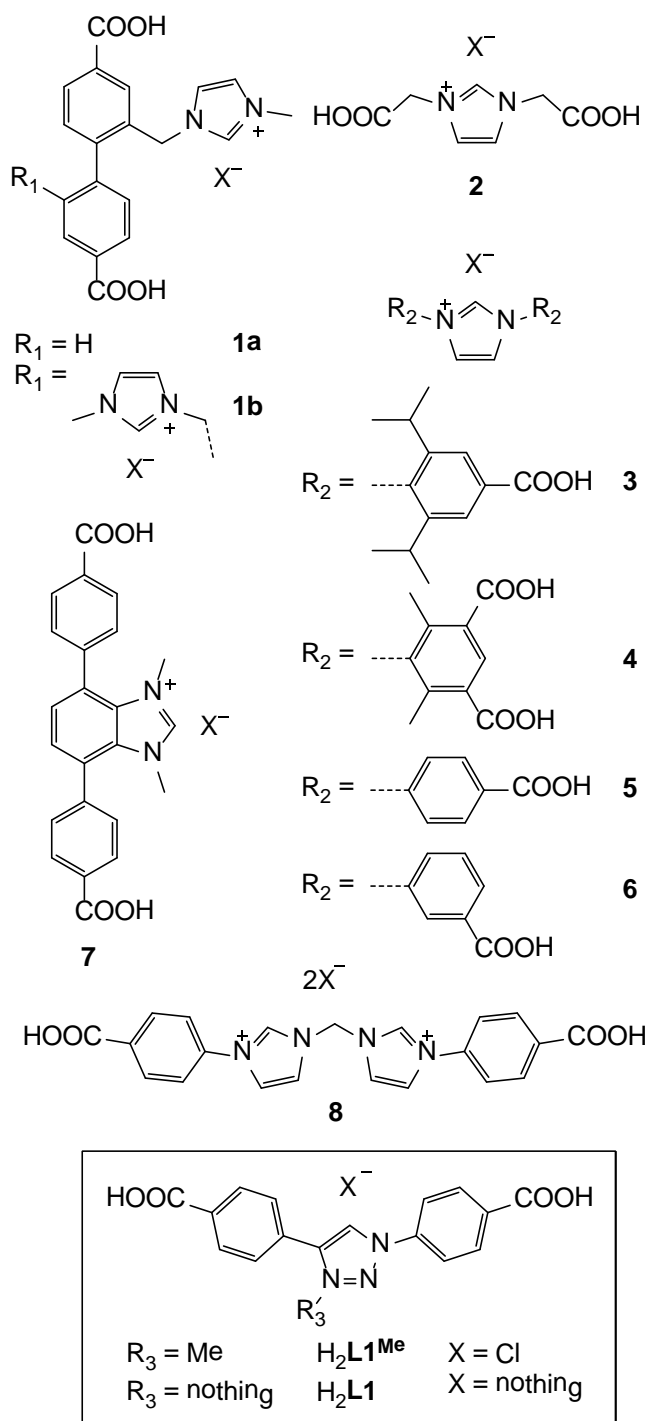
Figure 1. Reported examples of pendant (**1a**, **1b**, and **7**) and integrated (**3** – **6**, **8**) imidazolium links for MOFs.

The focus of this current contribution is the first report of integrated triazolium-containing linker with carboxylate donors and the first MOFs containing linkers of this type. The ability to incorporate a triazolium precursor versus an imidazolium link[9-11] offers an opportunity to tune the electronic and catalytic properties of the resulting N-heterocyclic carbene.[12] Herein we report the

synthesis of a novel triazolium link (**L1^Me**) *via* 'Click' chemistry and a comparison of the coordination chemistry for linkers containing a triazole (**L1**) or triazolium (**L1^Me**) core. We also investigate the control of interpenetration for a 2-D copper(II) MOF based on dicopper(II) paddlewheels and **L1^Me**.

Results & Discussion

*Ligand Synthesis*

Our previous dicarboxylate azolium ligands, 1,3-bis(4-carboxyphenyl)imidazolium bromide (**5**) and 1,3-bis(3-carboxyphenyl)imidazolium bromide (**6**) were synthesised by condensation of two equivalents on a cyanoaniline with glyoxal, cyclisation with paraformaldehyde to give the imidazolium, followed by acid catalysed hydrolysis using hydrobromic acid to the dicarboxylic acids.[9d] The synthesis of the triazolium equivalent of **5** was proposed to proceed via a copper(I)-catalyzed azide-alkyne cycloaddition or 'Click' reaction (Scheme 1). 'Click' chemistry has recently found application in a wide variety of areas[13] and a number of groups[14] have extensively exploited stepwise Huisgen cycloaddition reactions in triazole ligand synthesis. 1,4-Bis(methyl 4-benzoate)-1H-1,2,3-triazole (**9**) was synthesised using the general "Click reaction" procedure.[15] Equimolar amounts of methyl 4-ethynylbenzoate and methyl 4-azidobenzoate were reacted together in the presence of $CuSO_4 \cdot 5H_2O$ and sodium ascorbate in $EtOH/H_2O$ (7:3), and then heated under reflux for 16 h (Scheme 1). After workup, **9** was isolated in 92% yield as a pale beige powder. Of interest, when the reaction was carried out at room temperature for one week, both starting materials, the alkyne and the azide, were quantitatively recovered. This observation is consistent with the strong electron withdrawing effect of the CO_2Me group of the azide, which significantly slows down the rate of the Click reaction.[16] Surprisingly, **9** is insoluble in all common solvents at room temperature and can only solubilised when heated at 150°C in DMSO-d_6 which enabled "quick" ^1H NMR characterisation (no more than 2 transients) before recrystallising out upon cooling to room temperature. Methylation of **9** using trifluoromethane sulfonate in 1,1,2,2-

6

tetrachloroethane at 150°C afforded **10**(OTf) in quantitative yield (95%).[17] Finally, both biscarboxylic acid H$_2$**L1**(HCl) and H$_2$**L1**^{Me} as its chloride salt were obtained in excellent yield (82% and 85% respectively) by conventional deprotection of the methyl esters, refluxing **9** or **10**(OTf) in a 1:4 KOH(2M)/methanol mixture. Elemental analysis carried out on H$_2$**L1**(HCl) confirmed that H$_2$**L1** was isolated as its hydrochloride salt.
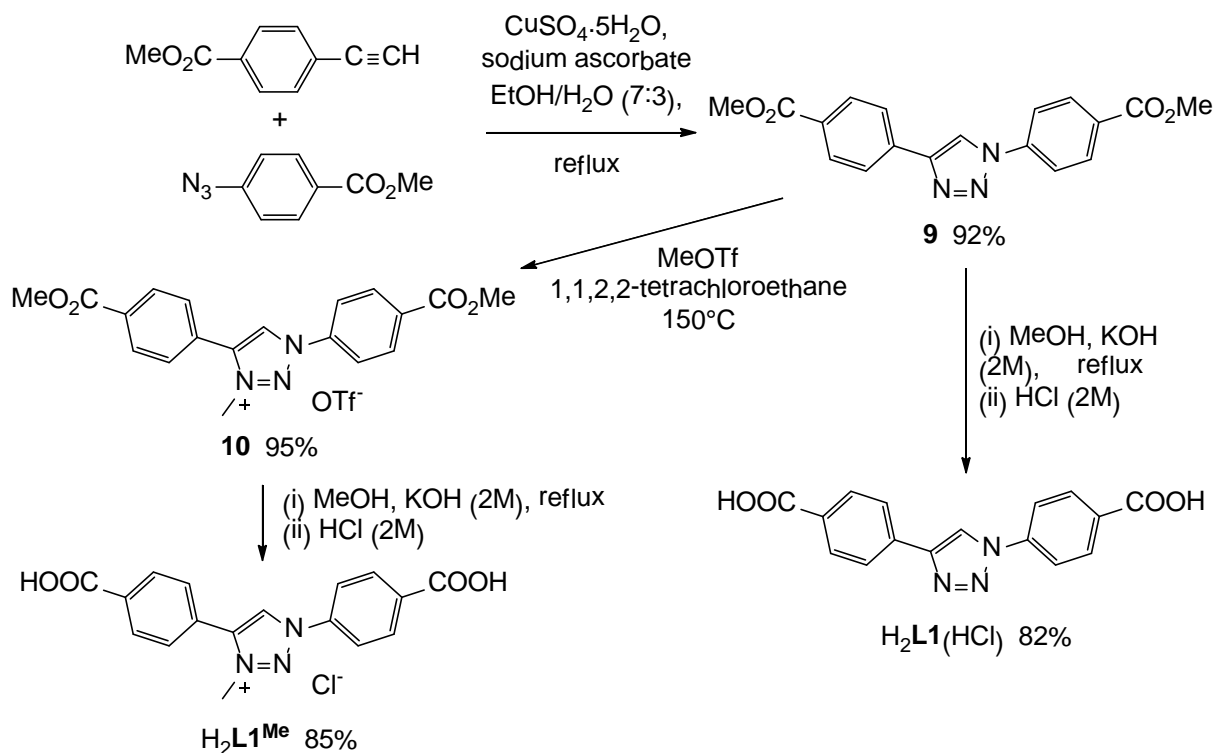
Scheme 1. Preparation of the triazole and triazolium ligands H$_2$**L1** and H$_2$**L1**^{Me}.

Compounds **9**, **10**(OTf), H$_2$**L1**(HCl) and H$_2$**L1**^{Me} were characterised by elemental analysis and the usual spectroscopic methods when achievable. Indeed, the low solubility of **9** and H$_2$**L1**(HCl) did not enable ^{13}C NMR and mass spectra to be recorded for these compounds. In the ^{1}H NMR spectra, the characteristic protons of the triazole and triazolium units can be found as singlets at ~9.6 and ~10.1 ppm for **9** or H$_2$**L1**(HCl) and **10**(OTf) or H$_2$**L1**^{Me}, respectively. For **10**(OTf) and H$_2$**L1**^{Me}, the ^{1}H NMR and ^{13}C NMR spectra confirmed that the methylation had successfully occurred (NCH$_3$: δ_H 4.49 for both **10**(OTf) and H$_2$**L1**^{Me}, δ_C 39.57 for **10**(OTf) and hidden in the residual solvent peak for H$_2$**L1**^{Me}). ^{1}H NMR spectroscopy also confirmed the successful

deprotection of the methyl esters by the lack of the CH_3 signals (found at δ 3.92, 3.89 and δ 3.94 in **9** and **10**(OTf) respectively) and the appearance of a characteristic broad singlet at δ 13.14 and 13.54 in H_2L1 and H_2L1^{Me} respectively, due to the carboxylic acid protons. In the IR spectra the C=O stretch shifted from ~ 1720 cm^{-1} for the diesters **9** and **10**(OTf), to 1681 and 1711 cm^{-1} for the dicarboxylic acids H_2L1 and H_2L1^{Me}, respectively. This was also accompanied by the appearance of a characteristic large and broad O-H stretch at ~3000 cm^{-1} for both dicarboxylic acids.

Crystal structure of HL1^{Me}·H$_2$O

Further confirmation of the successful synthesis of H_2L1^{Me} came from a single crystal X-ray crystal structure of $L1^{Me}$ as its zwitterion. Crystals of $HL1^{Me}$·H_2O were obtained from a 1:1 solution of $L1^{Me}$ in DMF/H_2O (1.6 mL) containing one drop of concentrated nitric acid. H_2L1^{Me} crystallises in the monoclinic space group $P2_1/c$ with one complete molecule in the asymmetric unit (Figure 2). The compound adopts the expected conformation with the phenyl rings twisted out of the plane of the triazolium core by 15.3(1) and 20.5(1)° and expected bond lengths and angles for such a compound.[9, 14] As was observed for previously reported integrated azolium links,[9e-g] the angle subtended by the two 4-carboxylate groups is 145.4(1) ° and consistent with the O-Si-O angle in zeolites. The structure confirms that the methylation of **L1** has taken place in the 3-position of the triazole to give H_2L1^{Me}. In the structure H_2L1^{Me} is found as a zwitterion with a water molecule hydrogen bonded to the triazolium CH (D_{CO} = 3.06, $d_{CH\cdots O}$ = 2.14 Å; angle = 162.0°).
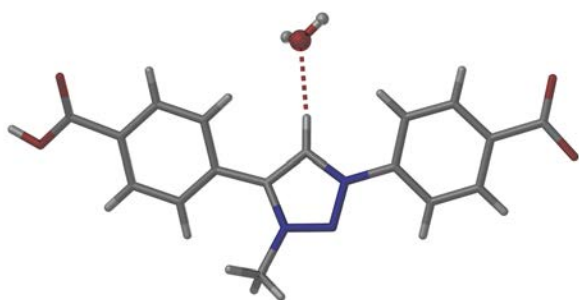
Figure 2. A view of a single molecule of **HL1^{Me}** showing the angle subtended by the two 4-carboxylate groups and the hydrogen bonded water molecule (ball and stick representation). The dashed bond represents a hydrogen bond with the acidic triazolium CH (D_{CO} = 3.06, $d_{CH\cdots O}$ = 2.14 Å; angle = 162.0°).

The packing of **HL1^{Me}** in the crystal is mediated by the formation of a strong hydrogen bond (D_{OO} = 2.47, $d_{OH\cdots O}$ = 1.56 Å; angle = 172.7°) between the protonated and the deprotonated carboxylates to form a 1-D tape of **HL1^{Me}**. The water solvate molecule acts as a three connecting centre to form three hydrogen bonding interactions with three different molecules of **HL1^{Me}**. The water molecule acts as a hydrogen bond donor to the deprotonated carboxylate of one molecule of **HL1^{Me}** (D_{OO} = 2.77, $d_{OH\cdots O}$ = 1.93 Å; angle = 167.0°) and to the carbonyl oxygen of a carboxylic acid in a second molecule (D_{OO} = 2.85, $d_{OH\cdots O}$ = 2.03 Å; angle = 165.8°). The third interaction is the acceptor interaction described above for the triazolium core. The combined interactions result in a 3-D hydrogen bonded network.

MOF synthesis

Due to the ease of access to a neutral analogue of **H$_2$L1^{Me}**, **H$_2$L1**, which will provide a dianionic rather than monoanionic ligand on deprotonation, we first examined the coordination chemistry of **H$_2$L1** with zinc(II) and copper(II) metal salts. Unfortunately, as noted above, **H$_2$L1** is remarkably insoluble. However, after screening a number of conditions, **H$_2$L1**(HCl), zinc nitrate and one drop of concentrated HNO$_3$ were reacted at 85°C for 2 days in a 1:1 DMF/ethanol solution. After washing the resulting crystals, this gave [Zn(**L1**)$_2$(H$_2$O)$_2$] (**11**) as a white crystalline powder in 39% yield. The phase purity and composition of the material was confirmed by Powder X-ray Diffraction (PXRD) (Figure SI 1), combustion analysis, and IR spectroscopy.

*Structure of [Zn(**L1**)$_2$(H$_2$O)$_2$] **11**.* [Zn(**L1**)$_2$(H$_2$O)$_2$] is a 2-D MOF formed from infinite chains of 5-coordinate zinc centres that extend along the *c*-axis and four-connecting molecules of **L1** that are directed along the *ac* diagonal (Figure 3(a)). The compound crystallises in the monoclinic space group *P*2$_1$/*c* with an asymmetric unit that contains a single molecule of **L1**, a zinc atom and a water molecule. Each zinc centre is coordinated to four carboxylate oxygen atoms from four separate molecules of **L1** (Zn1 O19 1.957(6), Zn1 O18 2.129(8)) and a water molecule (Zn1 O20 1.912(12)). The zinc(II) cations are best described as having a distorted five-coordinate geometry part way between trigonal bipyramidal and square planar with the water in the trigonal plane directed along the *b*-axis. In turn each ligand coordinates four separate zinc centres through monodentate coordination. Notably, the triazole nitrogens are not involved in coordination of the zinc atom. This may be due to a combination of factors, including sterics, the reaction stoichiometry, and a favourable hydrogen bonding interaction in the repeating structure as described below.
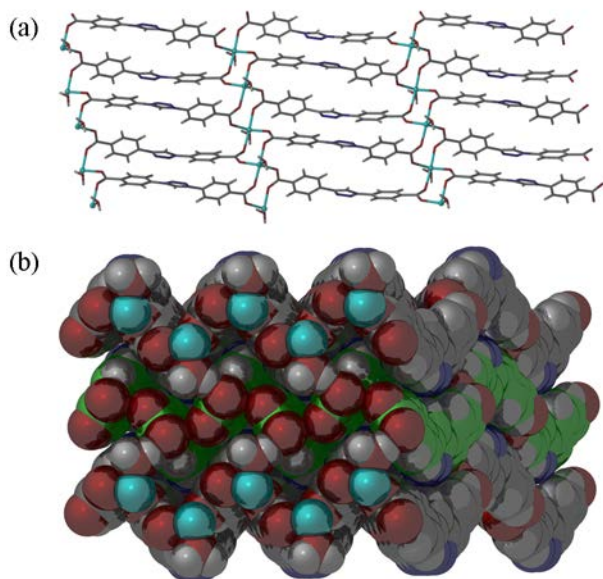

Figure 3. (a) A perspective view of the 2-D MOF structure in [Zn(**L1**)$_2$(H$_2$O)$_2$] **11** showing the infinite zinc bridging carboxylate chains running along the *c*-axis. (b) The close-packed 3-D structure of **11**. Multiple inter-sheet hydrogen bonds involving the carboxylate oxygens, the triazole moieties, and the coordinated water ligands stabilize the packing.

The 2-D sheets adopt a zig-zag conformation in the solid-state and within the crystal are close-packed to give a dense, non-porous 3-D hydrogen bonded network (Figure 3(b)). The crystal packing is mediated by inter-sheet hydrogen bonding interactions involving the triazole rings of adjacent 2-D MOFs which form hydrogen bonded tapes (D_{CN} = 3.71, $d_{CH\cdots N}$ = 2.78 Å; angle = 168.9°; D_{CN} = 3.71, $d_{CH\cdots N}$ = 2.86 Å; angle = 163.6°), as is commonly observed for triazoles,[14, 18] that are orthogonal to the 2-D MOF. Within the 2-D MOF the triazole ligands alternate orientation so the tapes run in both directions in the crystal. The inter-sheet bonding is supported by further strong hydrogen bonds involving the water ligands as hydrogen bond donors and the carboxylate oxygen atoms of adjacent chains as acceptors (D_{OO} = 2.62, $d_{OH\cdots O}$ = 1.76 Å; angle = 157.9°; D_{OO} = 2.61, $d_{OH\cdots O}$ = 1.77 Å; angle = 162.9°).

With poor solubility severely limiting the ability to form MOFs with H_2L1, we moved onto investigations involving H_2L1^{Me}. The triazolium compound is noticeably more soluble than H_2L1, and the methylation of the triazole ring prevents the formation of triazole $C-H\cdots N_{triazole}$ hydrogen bonding as a structure directing interaction. Thus, reaction with zinc(II) nitrate with H_2L1^{Me}, as reported above for H_2L1, does not lead to the formation of a structure isomorphous with **11**. However, reaction of H_2L1^{Me} with copper(II) nitrate in DMF did yield, after one night at 85°C, smaller and larger blue block shaped crystals that correspond to a mixture of catenation isomers of $[Cu_2(L1^{Me})_2(DMF)_2](NO_3)_2$; specifically a near close-packed three-fold interpenetrated isomer, α-$[Cu_2(L1^{Me})_2(DMF)_2](NO_3)_2$ (**12**), and a more open two-fold interpenetrated structure, β-$[Cu_2(L1^{Me})_2(DMF)_2](NO_3)_2$ (**13**). The formation of **12** (blue blocks) as the sole product was achieved by undertaking the reaction in DMF, containing one drop of concentrated HNO_3, at 85°C for 2 days. This was confirmed by PXRD (Figure 4) that showed an extremely good match between the calculated pattern for **12** and the experimental patterns for samples obtained from reactions undertaken in the presence of nitric acid. The formation of **12** was supported by elemental analysis (as a hydrate, $[Cu_2(L1^{Me})_2(H_2O)_2](NO_3)_2\cdot 1\frac{1}{2}H_2O$, after washing and drying under high vacuum).

Formation of the open structure as the sole product was more difficult. Indeed, when the reaction is carried out at higher temperature the percentage of **13** in the mixture of **12** and **13** increases, which was confirmed by the PXRD studies. However, it was difficult to isolate isomer **13** pure; the best conditions to obtain **13** as the major product being to undertake the reaction at 120°C for 1 day (Figure 4), although on certain attempts pure **13** (blue rods) was obtained as the sole product.
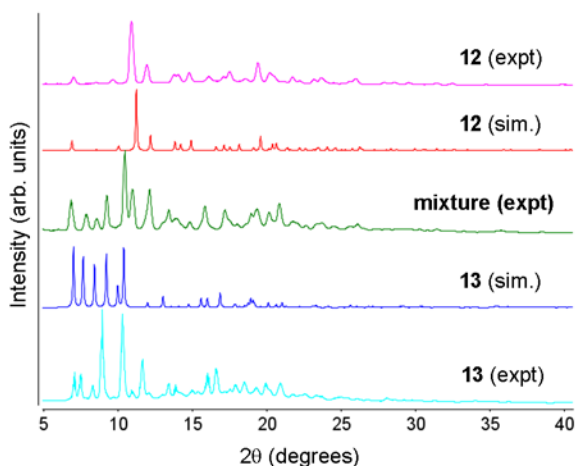

Figure 4 . Experimental PXRD patterns for α-[Cu_2($L1^{Me}$)$_2$(DMF)$_2$](NO$_3$)$_2$ (**12**, pink) and α-[Cu_2($L1^{Me}$)$_2$(DMF)$_2$](NO$_3$)$_2$ (**13**, aqua), and calculated PXRD patterns for **12** (red) and **13** (blue). The initial experimental PXRD of the mixture of **12** and **13** is shown in green.

*Structures of α- and β-[Cu ($L1^{Me}$)$_2$(DMF)$_2$](NO$_3$)$_2$ (**12** and **13**)*

Both **12** and **13** have a very similar 4-connected 2-D network structures based around dicopper(II) paddlewheel secondary building units (SBUs), however there are noticeable differences in the conformation of the 2-D MOF and in the solid-state packing. Contrary to previous observations,[19] compound (**12**), which is produced at lower temperatures or in the presence of acid that slows down the rate of reaction, is 3-fold interpenetrated, while the material grown more rapidly at higher temperatures (**13**) is only 2-fold interpenetrated. Previously Zaworotko,[19a] and more recently Matzger,[19b] showed the lower temperature phase was non-interpenetrated. Zaworotko rationalised this observation on the basis that the formation of the more thermodynamically stable product, i.e. a

denser interpenetrated structure, is favoured at higher temperatures. Given our current experimental observations we believe the synthesis of **12** and **13** is under kinetic control; thus higher temperatures and a shorter reaction time (1 day versus 3 days) lead to the formation of 2-fold interpenetrated **13** as the preferred product.

Compound **12** crystallises in the orthorhombic space group *Pbca* with a single copper(II) atom, a molecule of **L1^{Me}** and a DMF ligand in the asymmetric unit and a unit cell volume of 4235.4(4) Å^3. A perspective view of the 2-D MOF structure in **12** is shown in Figure 5(a). The dicopper(II) paddlewheel SBUs are typical[20] and the triazolium link maintains a geometry similar to that observed in the solid-state structure seen for **HL1^{Me}**·H$_2$O with an angle between the two carboxylate groups of 151.4° (compared with 145.4(1) ° in **HL1^{Me}**·H$_2$O). The distance bridged by the link (between the centroids of the paddlewheels) is 18.1(1) Å, although the angle subtended by the ligand and the twist relative to the plane of the 2-D MOF means the windows are not regular with width 15.1(1) Å and length 21.7(1) Å. This provides windows of roughly *ca.* 11.7 by 18.3 Å taking into account the van der Waal's radii. A similar topology was observed with the diazolium linker **8** and dicopper(II) paddlewheel SBUs[9h] and in the imidazolium structure reported by Son and co-workers.[9e]
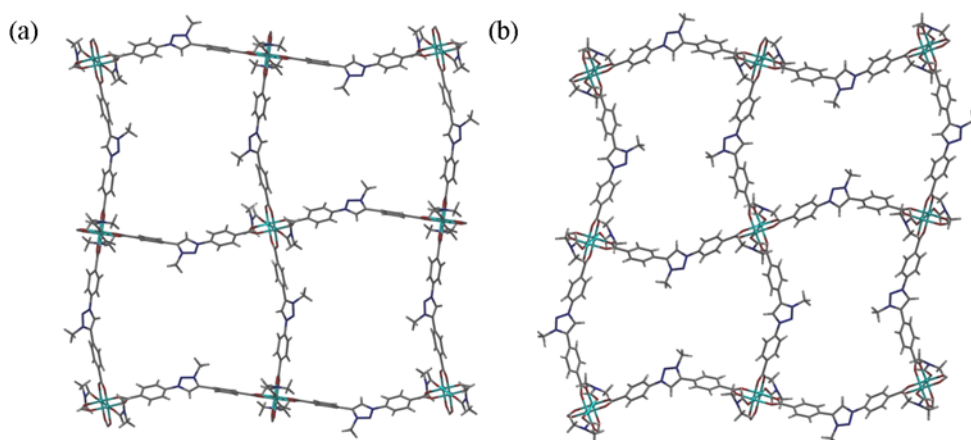

Figure 5. The 2-D MOFs in the structures of (a) **12** and (b) **13**.

13

Adjacent 2-D networks that are packed parallel to the original network (parallel to the *ac* diagonal) are offset by 9.4(1) Å and the DMF ligands on the dicopper(II) paddlewheels are interdigitated into the windows (Figure 6(a)). This creates small rectangular channels that are viewed along the *a*-axis (Figure 6(b)). Unfortunately this pore volume is not available to do chemistry as two further 2-D networks, which are packed perpendicular to the first network, are accommodated in the pore to give a 3-fold interpenetrated structure. This results in a 3-D mechanically interlocked structure (Figures 6(c) and (d)).
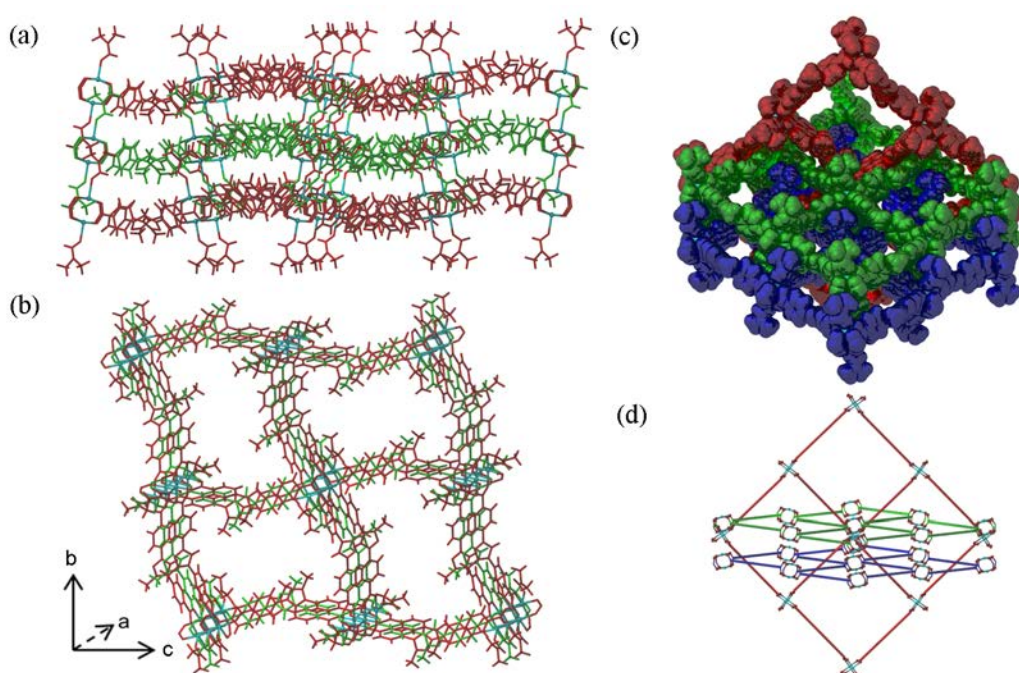
Figure 6. (a) A view of the packing of **12** showing the offset arrangement of the 2-D MOFs and the canting of the dicopper(II) paddlewheels. (b) A view down the *a*-axis and (c) the interpenetration of the 2-D grids (red) by two perpendicular layers (green and blue) to give a close-packed structure (hydrogen atoms omitted for clarity). (d) A simplified schematic of the interpenetrated structure.

Compound **13** also crystallises in an orthorhombic space group, but in *Pbcn* rather than *Pbca*, with a single copper(II) atom, a molecule of **L1^{Me}** and a DMF ligand in the asymmetric unit. The unit cell volume of **13** is considerably larger at 6101(2) Å^3 compared to **12** (4235.4(4) Å^3). While the nitrate anion could be observed in some data collections on the structure, in the final refinement

it could not be sensibly modelled and the SQUEEZE routine of PLATON[21] was applied to the collected data. A perspective view of the 2-D MOF structure in **13** is shown in Figure 5(b). The dicopper(II) paddlewheel SBUs are typical[20] and the triazolium link maintains a geometry similar to that observed in the solid-state structure seen for **HL1**$^{\text{Me}}$·H_2O and **12** with an angle between the two carboxylate groups of 147.2° (compared with 145.4(1) ° in **HL1**$^{\text{Me}}$·H_2O; 151.4° in **12**). The distance bridged by the link (between the centroids of the paddlewheels) is 17.9(1) Å, although the windows are not regular with width 12.9(1) Å and length 23.1(1) Å. This provides windows of roughly *ca.* 9.5 by 19.7 Å taking into account the van der Waal's radii. Thus the windows in the 2-D grid are more pinched widthways and slightly elongated lengthways compared to the windows in **12**.

In structure **13** adjacent 2-D networks, which are packed parallel to the original network (parallel to the *ab* diagonal), are slightly offset to accommodate the packing. In **13** the 2-D MOFs are planar and not undulating as observed in the structure of **12**. By comparison with **12** this creates large rectangular channels that are viewed along the *b*-axis (Figure 7(a)). In **13** only one 2-D network is accommodated in each window to give a 2-fold interpenetrated 3-D mechanically interlocked structure (Figure 7(b)). In this instance the networks are packed such that small triangular shaped channels with *ca.* 9.5(1) Å sides percolate down the *b*-axis.
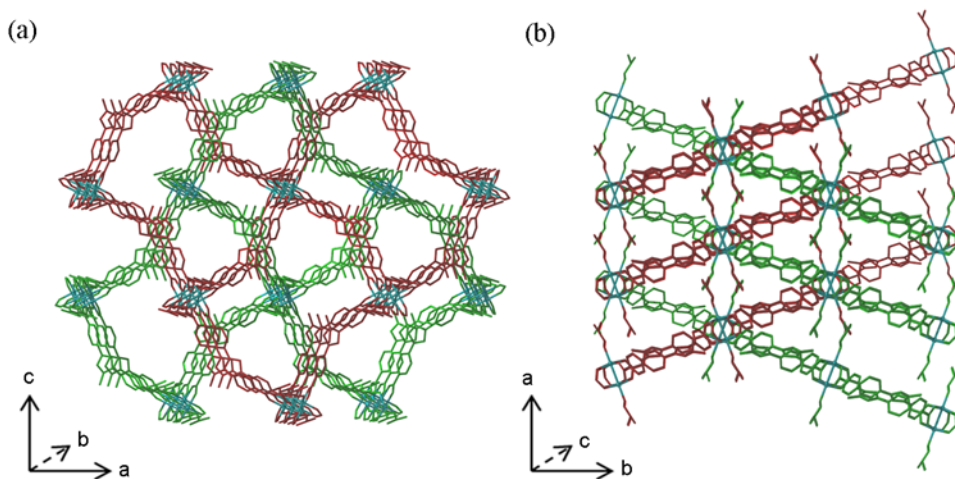
Figure 7. Views down (a) the *b*-axis and (b) the *c*-axis showing the 2-fold interpenetration (hydrogen atoms omitted for clarity). The approximately triangular channels that percolate along the *b*-axis are shown in (a).

Conclusion

This work describes the synthesis and structures of a series of MOFs made from novel triazole and triazolium based links. Due to exploitation of the well-developed Click reaction methodology triazolium links bearing appropriate donor groups can be synthesised in high yield via short synthetic pathways. Careful manipulation of the conditions was required to facilitate both the Click reaction in the presence of electron withdrawing substituents on the azide and the methylation step to overcome the poor solubility of the triazole diester **9**. We further demonstrate that subtle differences in the structure of the link, the choice of metal salt, and the conditions used for synthesis (temperature, additives) can have a dramatic effect on the net topology and degree of catenation. Current work in our laboratory is focused on using this knowledge to design new azolium links that will give rise to architectures with larger pore volumes that will facilitate the binding of known homogeneous catalytic moieties.

Experimental

General experimental

Melting points were measured on a Gallenkamp melting point apparatus and are uncorrected. Elemental analyses were performed by the Campbell Microanalytical Laboratory at the University of Otago. Infrared spectra were collected on a Perkin Elmer 100S Infrared spectrometer in Universal ATR mode. NMR spectra were recorded on a Varian Gemini 300 MHz or a 600 MHz NMR spectrometer at 23 °C using a 5 mm probe. ^{1}H (^{13}C) NMR spectra recorded in DMSO-d_6 were referenced to the solvent peak: 2.5 ppm (39.5 ppm). Electrospray (ES) mass spectra were recorded using a Finnigan LCQ mass spectrometer. Unless otherwise stated, all chemicals were obtained

from commercial sources and used as received. Methyl 4-ethynylbenzoate[22] and methyl 4-azidobenzoate[23] were prepared according to the methods described in the literature.

Synthesis

Synthesis of 1,4-Bis(methyl 4-benzoate)-1*H*-1,2,3-triazole, 9

To a stirred solution of methyl 4-ethynylbenzoate (351 mg, 2.19 mmol) and methyl 4-azidobenzoate (388 mg, 2.19 mmol) in EtOH/H_2O (25 mL, 7:3) was added $CuSO_4$ $5H_2O$ (109 mg, 0.44 mmol) and sodium ascorbate (174 mg, 0.88 mmol). The solution was then heated to the reflux point under nitrogen atmosphere for 16 hrs. After the reaction mixture was cooled down to room temperature, ammonia (75 mL, 14%) was added. The resulting precipitate was filtered off and washed well with H_2O, and then with dichloromethane (3×20 mL) to afford **9** as an insoluble pale beige powder (681 mg, 92%). Mp 298 °C. Anal. calcd ($C_{18}H_{15}N_3O_4$): C, 64.09; H, 4.48; N, 12.46. Found: C, 63.99; H, 4.41; N, 12.44. IR (powder): $\nu(CO_2Me)$ 1723 (s), $\nu(C=C)$ 1608 (m) cm^{-1}. ^{1}H NMR (DMSO-d_6, 300 MHz): δ 9.55 (s, 1H, H$_{triazole}$), 8.22-8.10 (m, 8H, H$_{aromatic}$), 3.92 (s, 3H, CH_3), 3.89 (s, 3H, CH_3).

Synthesis of 1,4-Bis(4-benzoic acid)-1*H*-1,2,3-triazole hydrochloride, H$_2$L1(HCl)

Potassium hydroxide solution (4 mL, 2 M) was added to a stirred solution of **9** (250 mg, 0.74 mmol) in methanol (16 mL). The reaction mixture was then heated to the reflux point for 16 hrs. After the reaction mixture cooled down to room temperature, HCl solution (2 M) was added dropwise until pH 1-2 was reached. The resulting precipitate was filtered off, washed well with H_2O, and dried under high vacuum to afford H$_2$**L1**(HCl) as a white powder (211 mg, 82%). Anal. calcd ($C_{16}H_{11}N_3O_4$ HCl): C, 55.58; H, 3.50; N, 12.15. Found: C, 56.79; H, 3.22; N, 12.29. IR (powder): $\nu(O-H)$ 2990 (s), $\nu(CO_2H)$ 1681 (s), $\nu(C=C)$ 1608 (m) cm^{-1}. ^{1}H NMR (DMSO-d_6, 600 MHz): δ 13.14 (s, 2H, CO_2H), 9.57 (s, 1H, H$_{triazole}$), 8.18-8.08 (m, 8H, H$_{aromatic}$). ^{13}C NMR (DMSO-d_6, 150 MHz): δ 166.90 (CO_2H), 166.33 (CO_2H), 146.62, 139.39, 134.07, 131.17-130.13 (m(br)), 125.34, 120.85, 119.79.

Synthesis of 1,4-Bis(methyl 4-benzoate)-1-methyl-1*H*-1,2,3-triazolium triflate, 10(OTf)

To a stirred solution of **9** (800 mg, 2.37 mmol) in well degassed 1,1,2,2-tetrachloroethane (40 ml) was added dropwise methyl triflate (0.54 mL, 4.74 mmol). The solution was then heated at 150°C for 16 hrs. After the reaction mixture cooled down to room temperature, the solution was filtered and then diethyl ether (150 mL) was added to the mixture. The resulting precipitate was filtered off and washed with diethyl ether (3×50 mL) to afford **10**(OTf) as a white powder (1.129 g, 95%). Anal. calcd ($C_{20}H_{18}F_3N_3O_7S_1$): C, 47.91; H, 3.62; N, 8.38. Found: C, 47.97; H, 3.46; N, 8.35. IR (powder): $\nu(CO_2Me)$ 1724 (s) cm^{-1}. ^{1}H NMR (DMSO-d_6, 600 MHz): δ 10.05 (s, 1H, H$_{triazolium}$), 8.35 (d, $^3J_{H-H}$ = 8.7 Hz, 2H, H$_{aromatic}$), 8.26 (m, 4H, H$_{aromatic}$), 8.01 (d, $^3J_{H-H}$ = 8.3 Hz, 2H, H$_{aromatic}$), 4.49 (s, 3H, NCH$_3$), 3.94 (s, 6H, CO$_2$CH$_3$). ^{13}C NMR (DMSO-d_6, 150 MHz): δ 165.38 (*C*O$_2$CH$_3$), 164.90 (*C*O$_2$CH$_3$), 142.33, 137.69, 132.38, 132.25, 131.39, 130.02, 129.83, 128.24, 126.67, 121.65, 52.72 (CO$_2$*C*H$_3$), 52.63 (CO$_2$*C*H$_3$), 39.57 (NCH$_3$). ES-MS (positive ion mode, MeOH, m/z): 352.3 [M$^+$].

Synthesis of 1,4-Bis(4-benzoic acid)-1-methyl-1*H*-1,2,3-triazolium chloride, H$_2$L1^{Me}

Potassium hydroxide solution (15 mL, 2 M) was added to a stirred solution of **10**(OTf) (978 mg, 1.95 mmol) in methanol (60 mL). The reaction mixture was then heated to the reflux point for 16 hrs. After the reaction mixture cooled down to room temperature and then filtered, HCl solution (2M) was added dropwise until pH 1-2 was reached. The resulting precipitate was filtered off, washed well with H$_2$O, and dried under high vacuum to afford H$_2$**L1**^{Me} as a white powder (597 mg, 85%). Anal. calcd ($C_{17}H_{13}N_3O_4$ H$_2$O): C, 59.82; H, 4.43; N, 12.31. Found: C, 59.86; H, 4.23; N, 12.26. IR (powder): ν(O-H) 2889 (s), $\nu(CO_2H)$ 1711 (s) cm^{-1}. ^{1}H NMR (DMSO-d_6, 300 MHz): δ 13.54 (s, 2H, CO$_2$H), 10.13 (s, 1H, H$_{triazolium}$), 8.32-8.22 (m, 6H, H$_{aromatic}$), 7.99 (d, $^3J_{H-H}$ = 8.0 Hz, 2H, H$_{aromatic}$), 4.49 (s, 3H, NCH$_3$). ^{13}C NMR (DMSO-d_6, 75 MHz): δ 166.40 (CO$_2$H), 165.91 (CO$_2$H), 142.45, 137.44, 133.66, 133.50, 131.44, 130.11, 129.71, 128.19, 126.30, 121.51. ES-MS

(positive ion mode, MeOH, m/z): 324.2 [M$^+$]. X-Ray quality crystals of HL1^{Me}·H$_2$O were obtained by heating a 1:1 DMF/H$_2$O solution (3 mL, containing one drop of concentrated HNO$_3$) of H$_2$L1^{Me} (5 mg) at 85°C overnight.

[Zn(L1)$_2$(H$_2$O)$_2$] (11)

H$_2$L1(HCl) (4 mg, 0.013 mmol) and zinc(II) nitrate (3.8 mg, 0.013 mmol) were sealed in a 20 mL glass vial with a Teflon-lined screw cap along with a 1:1 DMF/ethanol solution (4 mL) and one drop of conc. HNO$_3$. The mixture was heated at 85°C for 2 days, and then allowed to cool down to room temperature. The resulting crystals were washed with fresh DMF, dichloromethane and then dried under vacuum to afford **11** as a white crystalline powder (2 mg, 39%). Anal. calcd (C$_{16}$H$_{11}$N$_3$O$_5$Zn): C, 49.19; H, 2.84; N, 10.76. Found: C, 49.26; H, 2.73; N, 10.84. IR (powder): ν 3106 (s), 1603 (m), 1518 (m), 1398 (s) cm^{-1}.

α-[Cu$_2$(DMF)$_2$(L1^{Me})$_2$](NO$_3$)$_2$ (12) and β-[Cu$_2$(DMF)$_2$(L1^{Me})$_2$](NO$_3$)$_2$ (13)

Compound **12**: H$_2$L1^{Me} (5 mg, 0.014 mmol) and copper nitrate (3.2 mg, 0.014 mmol) were sealed in a 20 mL glass vial with a Teflon-lined screw cap along with a DMF solution (1.5 mL) and one drop of conc. HNO$_3$. The mixture was heated at 85°C for 3 days, and then allowed to cool down to room temperature. The resulting crystals were washed with fresh DMF, dichloromethane and then dried under vacuum to afford **12** as blue crystals (3 mg, 43% based on the hydrate). Anal. calcd (C$_{17}$H$_{14}$N$_4$O$_8$Cu 1½H$_2$O): C, 41.43; H, 3.48; N, 11.37. Found: C, 41.39; H, 3.30; N, 11.19. IR (powder): ν 3077 (s), 1605 (m), 1552 (m), 1379 (s) cm^{-1}.

Compound **13**: H$_2$L1^{Me} (5 mg, 0.014 mmol) and copper nitrate (3.2 mg, 0.014 mmol) were sealed in a 20 mL glass vial with a Teflon-lined screw cap along with a DMF solution (1.5 mL). The mixture was heated at 120°C for 1 day, and then allowed to cool down to room temperature. The resulting crystals were washed with fresh DMF and then dried under vacuum to afford predominantly **13** as blue needle shaped crystals. IR (powder): ν 3068 (s), 1653 (m), 1621 (m), 1384 (s) cm^{-1}.

X-Ray crystallography

Crystals were mounted under oil on nylon loops. X-ray diffraction data were collected at 150(2) K with (i) Mo-Kα radiation (λ = 0.71073 Å) using an Oxford Diffraction X-calibur single crystal X-ray diffractometer (HL1^{Me}·H$_2$O) or (ii) at the MX1 beamline of the Australian Synchrotron[24] (λ = 0.71073 Å; compounds **11**, **12** and **13**). Data sets were corrected for absorption using a multi-scan method, and structures were solved by direct methods using SHELXS-97[25] and refined by full-matrix least squares on F^2 by SHELXL-97,[26] interfaced through the program X-Seed.[27] In general, all non-hydrogen atoms were refined anisotropically and hydrogen atoms were included as invariants at geometrically estimated positions, unless specified otherwise in additional details below. Figures were produced using the program POV-Ray,[28] interfaced through X-Seed. Publication materials were prepared using CIFTAB.[29] Details of data collections and structure refinements are given below and in Table 1. CCDC 903866 - 903869 contain the supplementary crystallographic data for these structures. These data can be obtained free of charge from The Cambridge Crystallographic Data Centre via www.ccdc.cam.ac.uk/data_request/cif.

Specific details of the structure refinements

Compound HL1^{Me}·H$_2$O: The hydrogen atoms on the water solvate molecule and the carboxylic acid were located in the difference map. Due to the very short O···O distance (2.465 Å) between the carboxylic acid hydrogen bonded to its own parent carboxylate, the hydrogen atom was allowed to freely refine. The position of the hydrogen atom following refinement is very close to the centre point between the two oxygen atoms (O-H distance of 1.106 Å). This is consistent with the situation for a very strong hydrogen bond (Δ pK$_a$ ~ 0).[30]

Compound 11: The triazole ring of **L1** is disordered over two positions and both sites (N1 and C4) refined with 50% occupancy by carbon and 50% occupancy by nitrogen. EXYZ and EADP commands were employed.

Compound 12: A total of six DFIX restraints were used to maintain chemically sensible bond lengths and angles for the coordinated DMF molecule in the structure.

Compound 13: The nitrate anion could not be located probably in the difference map. Four DFIX restraints were used to maintain chemically sensible bond lengths and angles for the coordinated DMF molecule in the structure. The structure also contains disordered solvent molecules in the large channels that run along the *b*-axis. The SQUEEZE routine of PLATON[21] was applied to the collected data, which resulted in significant reductions in R_1 and wR_2 and an improvement in the GOF. R_1, wR_2 and GOF before SQUEEZE routine: 14.3%, 46.1% and 2.06; after SQUEEZE routine: 8.9%, 30.5% and 1.29. The contents of the solvent region calculated from the result of SQUEEZE routine (one nitrate anion per asymmetric unit) are represented in the unit cell contents of the crystal data.

Table 1. Crystal data and X-ray experimental data for H$\mathbf{L1^{Me}}$·H$_2$O, **11**, **12** and **13**.

Compound	H$\mathbf{L1^{Me}}$·H$_2$O	11	12	13
Empirical formula	C$_{17}$H$_{15}$N$_3$O$_5$	C$_{16}$H$_{11}$N$_3$O$_5$Zn	C$_{20}$H$_{19}$CuN$_5$O$_8$	C$_{20}$H$_{19}$CuN$_5$O$_8$
Formula weight	341.32	390.65	520.94	520.94
Crystal system	monoclinic	monoclinic	orthorhombic	orthorhombic
Space group	$P2_1$/c	$P2_1$/c	$Pbca$	$Pbcn$
a (Å)	6.0690(5)	16.432(3)	17.632(3)	25.182(5)
b (Å)	34.215(4)	11.630(2)	9.4690(19)	10.411(2)
c (Å)	7.1683(5)	7.6510(15)	25.544(5)	23.273(5)
α (º)	90	90	90	90
β (º)	93.316(7)	94.39(3)	90	90
γ (º)	90	90	90	90
Volume (Å^3)	1468.0(2)	1457.9(5)	4264.8(14)	6101(2)
Z	4	4	8	8
Density (calculated) (Mg/m^3)	1.526	1.780	1.623	1.134
Absorption coefficient (mm^{-1})	0.115	1.721	1.084	0.758
F(000)	712	792	2136	2136
Crystal size (mm^3)	0.47x0.22x0.07	0.13x0.09x0.02	0.08x0.07x0.07	0.18x0.11x0.04
Theta range (º)	2.91 – 29.17	2.15 – 27.10	1.97 – 27.12	2.29 – 26.84
Reflections collected	13276	21972	63628	88763
Independent reflections	3555	3161	4671	6460
Observed reflections [I>2σ(I)]	2646	3019	3998	5102
Goodness-of-fit on F^2	1.061	1.057	1.655	1.292
R$_1$ [I>2σ(I)]	0.0563	0.0342	0.0986	0.0888
wR$_2$ (all data)	0.1324	0.0903	0.3505	0.3052

Accessory publications

Powder X-ray Diffraction Data for compound **11** is available from the journal's website.

Acknowledgements

References

[1]   (a) S. Kitagawa, R. Kitaura, S.-I. Noro, *Angew. Chem. Int. Ed.*, **2004**, *43*, 2334; (b) G. Ferey, *Chem. Soc. Rev.*, **2008**, *37*, 191; (c) R. Robson, *Dalton Trans.*, **2008**, 5113; (d) S.R. Batten, S.M. Neville, D.R. Turner, Coordination Polymers: Design, Analysis and Application, Royal Society of Chemistry, Cambridge (2009) p. 471.

[2]   (a) M. Eddaoudi, J. Kim, N. L. Rosi, D. T. Vodak, J. Wachter, M. O'Keeffe, O. M. Yaghi, *Science*, **2002**, *295*, 469; (b) H. Deng, C. J. Doonan, H. Furukawa, R. B. Ferreira, J. Towne, C. B. Knobler, B. Wang, O. M. Yaghi, *Science*, **2010**, *327*, 846; (c) N. Stock, S. Biswas, *Chem. Rev.*, **2012**, *112*, 933.

[3]   (a) A. Corma, H. Garcia, F. X. Llabres, I. Xamena, *Chem. Rev.*, **2010**, *110*, 4607; (b) L. Ma, C. Abney, W. Lin, *Chem. Soc. Rev.*, **2009**, *38*, 1248; (c) A. U. Czaja, N. Trukhan, U. Müller, *Chem. Soc. Rev.*, **2009**, *38*, 1284; (d) J. Lee, O. K. Farha, J. Roberts, K. A. Scheidt, S. T. Nguyen, J. T. Hupp, *Chem. Soc. Rev.*, **2009**, *38*, 1450.

[4]   (a) E. D. Bloch, D Britt, C. Lee, C. J. Doonan, F. J. Uribe-Romo, H. Furukawa, J. R. Long, O. M. Yaghi, *J. Am. Chem. Soc.*, **2010**, *132*, 14382; (b) C. J. Doonan, W. Morris, H. Furukawa, O. M. Yaghi, *J. Am. Chem. Soc.*, **2009**, *131*, 9492; (c) T. Jacobs, R. Clowes, A. I. Cooper, M. J. Hardie, *Angew. Chem. Int. Ed.*, **2012**, *51*, 5192.

[5]   (a) C. Wang, Z. Xie, K. E. deKrafft, W. Lin, *J. Am. Chem. Soc.*, **2011**, *133*, 13445; (b) P. V. Dau, M. Kim, S. J. Garibay, F. H. L. Muench, C. E. Moore, S. M. Cohen, *Inorg. Chem.*, **2012**, *51*, 5671; (c) P. V. Dau, M. Kima, S. M. Cohen, *Chem. Sci.*, **2012**, DOI: 10.1039/c0xx00000x.

[6]   A. J. Nuñez, L. N. Shear, N. Dahal, I. A. Ibarra, J. Yoon, Y. K. Hwang, J.-S. Chang, S. M. Humphrey, *Chem. Commun.*, **2011**, *47*, 11855.

[7]   (a) J. S. Seo, D. Whang, H. Lee, S. I. Jun, J. Oh, Y. J. Jeon, K. Kim, *Nature*, **2000**, *404*, 982; (b) B. Chen, L. Wang, Y. Xiao, F. R. Fronczek, M. Xue, Y. Cui, G. Qian, *Angew. Chem. Int. Ed.*, **2009**, *48*, 500; (c) X.-P. Zhou, Z. Xu, M. Zeller, A. D. Hunter, *Chem. Commun.*, **2009**, 5439.

[8]   (a) C.-D. Wu, A. Hu, L. Zhang, W. Lin, *J. Am. Chem. Soc.,* **2005**, *127*, 8940; (b) K. L. Mulfort, O. K. Farha, C. L. Stern, A. A. Sarjent, J. T. Hupp, *J. Am. Chem. Soc.*, **2009**, *131*, 3866; (c) T. Devic, P. Horcajada, C. Serre, F. Salles, G. Maurin, B. Moulin, D. Heurtaux, G. Clet, A. Vimont, J-M, Greneche, B. Le Ouay, F. Moreau, E. Magnier, Y. Filinchuk, J. Marrot, J-C, Lavalley, M. Daturi, G. Ferey, *J. Am. Chem. Soc.*, **2010**, *132*, 1127; (d) K. S. Jeong, Y. B. Go, S. M. Shin, S. J. Lee, J. Kim, O. M. Yaghi, N. Jeong, *Chem. Sci.*, **2011**, *2*, 877; (e) D. Rankine, A. Avellaneda, M. R. Hill, C. J. Doonan, C. J. Sumby, *Chem. Commun.* **2012**, *48*, 10328.

[9]   (a) Z. Fei, T. D. Geldbach, D. Zhao, R. Scopelliti, P. J. Dyson, *Inorg. Chem.*, **2005**, *44*, 5200; (b) Z. Fei, T. D. Geldbach, D. Zhao, R. Scopelliti, P. J. Dyson, *Inorg. Chem.*, **2006**, *45*, 6331; (c) L. Han, S. Zhang, Y. Wang, X. Yan, X. Lu, *Inorg. Chem.*,

2009, *48*, 786; (d) R. S. Crees, M. L. Cole, L. R. Hanton, C. J. Sumby, *Inorg. Chem.*,
2010, *49*, 1712; (e) J. Chun, I. G. Jung, H. J. Kim, M. Park, M. S. Lah, S. U. Son,
Inorg. Chem., **2009**, *48*, 6353; (f) J. Chun, H. S. Lee, I. G. Jung, S. W. Lee, H. J. Kim,
S. U. Son, *Organometallics*, **2010**, *29*, 1518; (g) J. Y. Lee, J. Roberts, O. K. Farha, J.
T. Hupp, K. A. Scheidt, *Inorg. Chem.* **2009** *48*, 9971; (h) G.-Q. Kong, X. Xu, C. Zou,
C.-D. Wu, *Chem. Commun.,* **2011**, *47*, 11005.

[10]   J. M. Roberts, O. K. Farha, A. A. Sarjeant, J. T. Hupp, K. A. Scheidt, *Cryst. Growth
Des.*, **2011**, *11*, 4747.

[11]   K. Oisaki, Q Li, H. Furukawa, A. U. Czaja, O. M. Yaghi, *J. Am. Chem. Soc.* **2010**,
132, 9262.

[12]   (a) J. R. Struble, J. W. Bode, *Tetrahedron*, **2008**, *64*, 6961; (b) J. R. Struble, J.
Kaeobamrung, J. W. Bode, *Org. Lett.*, **2008**, *10*, 957.

[13]   (a) H. C. Kolb, M. G. Finn, and K. B. Sharpless, *Angew. Chem. Int. Ed.*, **2001**, *40*,
2004; (b) J. E. Moses, A. D. Moorhouse, *Chem. Soc. Rev.* **2007**, *36*, 1249; (c) M. G.
Finn, V. V. Fokin, *Chem. Soc. Rev.*, **2010**, *39*, 1231.

[14]   (a) J. D. Crowley, A.-L. Lee, K. J. Kilpin, *Aust. J. Chem.*, **2011**, *64*, 1118; (b) J. D.
Crowley, D. A. McMorran, in "Click Triazoles" Topics in Heterocyclic Chemistry,
ed. J. Košmrlj, Springer Berlin, Heidelberg, **2012**, vol. 28, pp. 31; (c) D.
Schweinfurth, N. Deibel, F. Weisser and B. Sarkar, *Nachr. Chem.*, **2011**, *59*, 937; (d)
H. Struthers, T. L. Mindt, R. Schibli, *Dalton Trans.*, **2010**, *39*, 675; (e) S. O. Scott, E.
L. Gavey, S. J. Lind, K. C. Gordon, J. D. Crowley, *Dalton Trans.*, **2011**, *40*, 12117;
(f) K. J. Kilpin, U. S. D. Paul, A.-L. Lee, J. D. Crowley, *Chem. Commun.*, **2011**, *47*,
328; (g) K. J. Kilpin, E. L. Gavey, C. J. McAdam, C. B. Anderson, S. J. Lind, C. C.
Keep, K. C. Gordon, J. D. Crowley, *Inorg. Chem.*, **2011**, *50*, 6334.

[15]   V. V. Rostovtsev, L. G. Green, V. V. Fokin, K. B. Sharpless, *Angew. Chem., Int. Ed.* **2002**, *41*, 2596.

[16]   A. R. Katritzky, Y. Zhang, S. K. Singh, *Heterocycles*, **2003**, *60*, 1225.

[17]   G. Guisado-Barrios, J. Bouffard, B. Donnadieu, G. Bertrand, *Organometallics*, **2011**, *30*, 6017.

[18]   (a) Y. Hua, A. H. Flood, *Chem. Soc. Rev.*, **2010**, *39*, 1262; (b) A. D. Pehere, C. J. Sumby, A. D. Abell, *Org. Biomol. Chem.*, **2012**, DOI: 10.1039/c2ob26637g.

[19]   (a) J. Zhang, L. Wojtas, R. W. Larsen, M. Eddaoudi, M. J. Zaworotko, *J. Am. Chem. Soc.*, **2009**, *131*, 17040; (b) J. I. Feldblyum, A. G. Wong-Foy, A. J. Matzger, *Chem. Commun.*, **2012**, *48*, 9828.

[20]   (a) M. Eddaoudi, D. B. Moler, H. Li, B. Chen, T. M. Reineke, M. O'Keeffe, O. M. Yaghi, *Acc. Chem. Res.*, **2001**, *34*, 319; (b) D. J. Tranchemontagne, J. L. Mendoza-Cortés, M.l O'Keeffe, O M. Yaghi, *Chem. Soc. Rev.*, **2009**, *38*, 1257.

[21]   A. L. Spek, *Acta Cryst.*, **1990**, *A46*, C34.

[22]   W. B. Austin, N. Bilow, W. J. Kelleghan, K. S. Y. Lau, *J. Org. Chem.*, **1981**, *46*, 2280.

[23]   M. Tanno, S. Sueyoshi, S. Kamiya, *Chem. Pharm. Bull.*, **1982**, *30*, 3125.

[24]   T. M. McPhillips, S. E. McPhillips, H. J. Chiu, A. E. Cohen, A. M. Deacon, P. J. Ellis, E. Garman, A. Gonzalez, N. K. Sauter, R. P. Phizackerley, S. M. Soltis, P. Kuhn, *J. Synchrotron Rad.*, **2002**, *9*, 401.

[25]   G. M. Sheldrick, *Acta Cryst.*, **1990**, *A46*, 467.

[26]   G. M. Sheldrick, *SHELXL-97*, University of Göttingen, Göttingen, Germany, **1997**.

[27]   L. J. Barbour, *J. Supramol. Chem.*, **2001**, *1*, 189.

[28]   Persistence of Vision Raytracer Pty. Ltd, *POV-Ray*, Williamstown, Australia, **2003-2008**.

[29]   G. M. Sheldrick, *CIFTAB*, University of Göttingen, Göttingen, Germany, **1997.**

[30]   P. Gilli, L. Pretto, V. Bertolasi, G. Gilli, *Acc. Chem. Res.*, **2009**, *42*, 33.